Adsorption of 2-Aminobenzothiazole on Colloidal Silver Particles: An Experimental and Theoretical Surface-Enhanced Raman Scattering Study

Jyotirmoy Sarkar,[†] Joydeep Chowdhury,[‡] Manash Ghosh,[†] Rina De,[§] and G. B. Talapatra*[,†]

Department of Spectroscopy, Indian Association for the Cultivation of Science, Jadavpur, Kolkata 700 032, Department of Physics, Sammilani Mahavidyalaya, Baghajatin Station, E.M. Bypass, Kolkata 700 075, and Department of Physics, Raja Rammohan Ray Mahavidyalaya, P.O. Nagulpara, Hooghly 712 406, India

Received: February 8, 2005; In Final Form: April 11, 2005

Surface-enhanced Raman scattering (SERS) spectra of the biologically important 2-aminobenzothiazole (2-ABT) molecule adsorbed on silver hydrosols are compared with its FTIR spectrum and normal Raman spectroscopy (NRS) spectrum in the bulk and in solution. The optimized structural parameters and the computed vibrational wavenumbers of the compound have been estimated from ab initio (Hatree−Fock) and density functional calculations. Some vibrational modes of the molecule have been reassigned. Concentration-dependent SERS spectra of the molecule reveal the existence of two types of vertically adsorbed species on colloidal silver particles, whose relative population varies with the adsorbate concentrations. The adsorption geometry and structural parameters of one type of adsorbed species are related to the NRS spectrum of the chemically prepared and theoretically modeled 2-ABT−Ag(I) coordination compound.

1. Introduction

Surface-enhanced Raman scattering (SERS) spectroscopy is a well-established and highly effective technique of observing Raman scattering from species present at trace concentrations.[1,2] It is a useful tool in surface chemistry because of its high sensitivity and potential in providing useful information regarding metal−adsorbate interactions.[3,4] The adsorptive site/sites and the orientation of the adsorbed molecule can be determined qualitatively by comparing the relative intensities and positions of the bands in the SERS spectrum with those in the Raman spectrum of the pure or solvated analyte.[5−7] Recently ab initio and density functional theory (DFT) were successfully utilized to model the experimentally observed SERS spectra.[8−10] The theoretical understanding of SERS, though not definite and still evolving, principally falls into two distinct concepts.[11,12] One is the electromagnetic contribution that attributed to the increase in the local field of the adsorbate due to excitation of the surface plasmons on the metal surface.[13−15] The other is the chemisorption, which is attributed to the short-distance chemical effect due to charge transfer (CT) between the metal and the adsorbed molecule.[16,17] Recently the role of charge transfer in the Raman enhancement process has been concluded by Haran et al.[18] from the time-dependent single-molecule Raman scattering study. They reported the SERS spectra of a single rhodamine 6G molecule, which showed dramatic fluctuation of the relative intensities of particular vibrational bands with time.

The compounds containing a thiazole ring have shown useful biological properties and have been developed as fungicides, herbicides, or plant growth regulators.[19] The biological importance of thiazole derivatives was emphasized during the period 1941−1945, when research on the structure of the antibiotic penicillin etc. showed the presence of a thiazolidine ring in this important therapeutic agent.[20] The 2-aminobenzothiazole (2-ABT) molecule is known for its local anaesthetic action and has numerous applications in human and veterinary medicine.[21] It is a metabolite of methabenzthiazuron[22] and is reported to form the main fraction of soil-bound residues.[23]

Considering the enormous biological importance, we present here the detailed experimental and theoretical normal Raman spectroscopy (NRS), SERS, and FTIR spectra of the 2-ABT molecule. The adsorptive behavior of 2-ABT on a colloidal silver surface at different adsorbate concentrations, close to that encountered under physiological conditions in living systems, has been elucidated from the SERS spectra. NRS spectra of the chemically prepared 2-ABT−Ag(I) complex and their comparison with the SERS spectra are also reported herein.

2. Experimental Section

2.1. Chemicals and Procedure. 2-ABT was purchased from Aldrich Chemical Co. and used without further purification. The molecule is readily soluble in acetonitrile solution. Stable silver sol was prepared by the process of Creighton et al.[24] The stable yellow sol thus prepared shows a single extinction maximum at 392 nm and was aged for two weeks before being used in the experiment. The size of the silver particles in this sol is known to be in the range 1−50 nm.[4,6,7] All required solutions were prepared with distilled and deionized water from a Milli-Q-plus system of M/S Millipore Corp. Mixing a specific volume of stock solution in acetonitrile with an appropriate volume of silver hydrosol attained the desired concentration of 2-ABT in silver hydrosol.

The 2-ABT−Ag(I) coordination compound was prepared according to the procedure reported by Dash et al.[25] It was prepared by reacting an aqueous solution of silver(I) nitrate with a hot aqueous solution of 2-ABT in a 1:2 stoichiometric ratio. The resulting mixture was then shaken for 15 min, resulting in the formation of a faint yellow crystalline compound. The compound was then filtered under suction, washed in ethanol

* To whom correspondence should be addressed. Phone: +91-33 24734971. Fax: +91-33 24732805. E-mail: spgbt@iacs.res.in.
[†] Indian Association for the Cultivation of Science.
[‡] Sammilani Mahavidyalaya.
[§] Raja Rammohan Ray Mahavidyalaya.

10.1021/jp050679z CCC: $30.25 © 2005 American Chemical Society
Published on Web 06/15/2005

and ether, and then dried in a vacuum. The complex so formed was insoluble in acetone and benzene but was fairly soluble in acetronitrile.

2.2. Instrumentation. Raman spectra were recorded by a Spex double monochromator (model 1403) fitted with a holographic grating of 1800 grooves/mm and a cooled photomultiplier tube (model R928/115) from Hamamatsu Photonics, Japan. The sample was taken in a quartz cell and was excited by 514.5 nm radiation from a Spectra Physics Ar^+ ion laser (model 2020-05) at a power of 200 mW. Raman scattering was collected at a right angle to the excitation. The operation of the photon counter and data acquisition and analysis were controlled by Spex Datamate 1B. The acquisition time by the spectral element was 0.5 s. The scattered light was focused onto the entrance slit of width 4 cm^{-1}. Polarized Raman spectra were recorded with an arrangement provided with the instrument. The accuracy in the measurement was ± 1 cm^{-1} for strong and sharp bands and slightly less for other bands. The FTIR spectra of the powder samples were taken in a KBr pellet using a Nicolet Magna-IR 750 spectrometer series II. The resolution of the infrared bands was about 4 cm^{-1} for sharp bands and slightly less for broader bands. All the spectra reported in the figures are original raw data directly transferred from the instrument and processed using the Microcal Origin version 6.0. They are presented even without single smoothing.

3. Theoretical Calculations

The theoretical calculations were carried out using the Gaussian 98 program for Windows.[26] Optimization of the molecular structures and the calculations of the vibrational frequencies for the optimized structures were done by the restricted Hartree−Fock (RHF) and density functional theory methods. The BPW91 functional[27] was used for the DFT calculations. The Pople split valance basis set[28] (except for the models of the surface complex) 6-31G(d,p) and Lanl2DZ were chosen in all the methods. For the 2-ABT−Ag(I) complex, a model in which 2-ABT interacts with Ag^+ through the N_9 atom was adopted. Calculations of the model for the Ag−molecule complex were performed using the combination of RHF/Lanl2DZ and BPW91/Lanl2DZ levels of theory. The Hartree−Fock frequencies were scaled by the scaling factor 0.8892,[29] but for the frequencies obtained with the BPW91 functional along with the Lanl2DZ basis set, satisfactory agreements between calculated and observed vibrational wavenumbers were obtained, without using a scaling factor. In the process of geometry optimization for the fully relaxed method, convergence of all the calculations and the absence of imaginary values in the wavenumbers confirmed the attainment of local minima on the potential energy surface.

4. Results and Discussion

4.1. Normal Raman and FTIR Spectra of 2-ABT and Their Vibrational Assignment. The 2-ABT molecule has 16 atoms; hence, it has 42 fundamental vibrations. It belongs to the C_s point group, and under this symmetry the 42 fundamental vibrations of the molecule are classified as

$$\Gamma_{vib} = 29\ A' + 13\ A''$$

Simple group theory predicts that 29 planar (A′) and 13 nonplanar (A″) species are expected to appear both in the Raman and in the IR spectra. The chemical structure of 2-ABT is shown in Figure 1. Selected optimized structural parameters of the free and adsorbed 2-ABT molecule calculated by the DFT and RHF

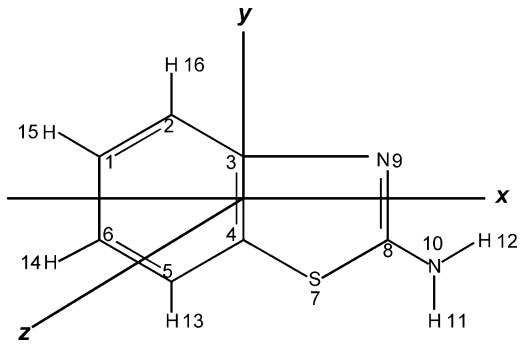

Figure 1. Schematic representation of the 2-aminobenzothiazole molecule.

ab initio methods are listed in Table 1. To the best of our knowledge, no X-ray crystallographic data of this molecule have yet been established. However, the theoretical results obtained by various methods are almost comparable with the recently reported structural parameters of the parent benzothiazole molecule.[30]

The normal Raman spectra of 2-ABT in 0.1 M solution and in neat solid are shown in part a and b, respectively, of Figure 2. The calculated NRS spectrum is shown in Figure 2c. It is to be emphasized that the calculated Raman spectrum represents the vibrational signatures of molecules in their gas phase. Hence, the experimentally observed Raman spectrum of the solid and solution may differ significantly from the calculated spectrum.[8] Despite this fact, one can see that there is a general concordance regarding the Raman intensities as well as the positions of the peaks between the experimental and calculated spectra.[9,31−33] The FTIR spectrum of the powdered sample in a KBr pellet is shown in Figure 3. Table 2 lists the FTIR, NRS, and SERS band frequencies of the molecule along with their tentative assignments and probable Raman polarizability tensor elements. The observed and calculated vibrational frequencies of the 2-ABT−Ag(I) complex are also shown in Table 2. In assigning the vibrational frequencies, the literature concerning the normal coordinate analysis and vibrational assignment of this[34] and related molecules[35−41] has been consulted.

The modes arising from the stretching and bending vibrations of the benzene and thiazole moieties of 2-ABT along with the scissoring mode of the externally attached $-NH_2$ group are identified. An interesting observation can be drawn regarding assignment of the band centered at ~1015 cm^{-1}. This band is intense and strongly polarized in the NRS spectra but appears as weak but prominent in the FTIR spectra. It principally represents a planer mode and has now been assigned to the ring breathing (ν_1) vibration of the benzene moiety.[42] Previously this band was ascribed to the C−C−C trigonal bending.[38] There is a discrepancy in the assignment of another band centered at 747 cm^{-1}. This band is very strong in the FTIR spectra but weak in the NRS spectra of the solid. Generally out-of-plane modes appear strong in the infrared and weak in the Raman,[6,43] so from this point of view, its earlier assignment as C−H out-of-plane bending is more justified.[32,38,40] However, this band is moderately intense in the NRS spectra of the solution and is polarized. The band has been reassigned, and considering the frequency region, it is thought to arise from one of the C−C−C trigonal in-plane bends (ν_{12}) of the fused benzene moiety of the 2-ABT molecule.[42]

4.2. Concentration-Dependent SERS Spectra of 2-ABT. Parts a−e of Figure 4 show the normalized SERS spectra of the 2-ABT molecule at varied adsorbate concentrations in the range 1.0×10^{-3} to 1.0×10^{-7} M. For each reduction of

TABLE 1: Relevant Structural Parameters of 2-ABT and the Changes Therein upon Binding to Ag at the RHF and DFT Levels of Theory

	RHF			DFT		
	2-ABT	2-ABT−Ag	diff	2-ABT	2-ABT−Ag	diff
			Bond Lengths (Å)			
C_2-C_3	1.3899	1.3917	−0.0018	1.4079	1.4109	−0.0030
C_3-C_4	1.3943	1.3952	−0.0009	1.4277	1.4220	0.0057
C_4-S_7	1.7562	1.8065	−0.0503	1.7675	1.8343	−0.0668
C_8-S_7	1.7648	1.7972	−0.0324	1.8022	1.8249	−0.0227
C_8-N_9	1.2707	1.3087	−0.0380	1.3068	1.3466	−0.0398
C_3-N_9	1.3872	1.4230	−0.0358	1.3888	1.4263	−0.0375
			Interatomic Angles (deg)			
$C_2-C_3-C_4$	119.30	119.53	−0.230	118.68	119.74	−1.06
$C_3-C_4-S_7$	108.77	109.99	−1.22	109.26	110.48	−1.22
$C_4-S_7-C_8$	88.03	87.99	0.04	87.73	87.93	−0.20
$C_3-N_9-C_8$	110.88	112.54	−1.66	110.41	113.46	−3.05
$S_7-C_8-N_9$	116.56	115.01	1.55	116.46	114.17	2.29
$C_2-C_3-N_9$	124.96	126.01	−1.05	125.18	126.31	−1.13
$C_1-C_2-C_3$	119.02	118.95	1.07	119.41	118.81	0.60
			Dihedral Angles (deg)			
$C_5-C_4-C_3-N_9$	179.43	179.99	−0.56	179.99	179.99	0 00

concentration of molecules in the silver sol, the concentration of acetonitrile (ACN) was kept constant, facilitating normalization of the SERS spectra. The normalization was done with respect to the 921 cm^{-1} band of ACN. It is established that ACN bands do not show any surface enhancement in the silver hydrosol,[44] so any possible interaction of ACN with the silver colloid can be neglected.

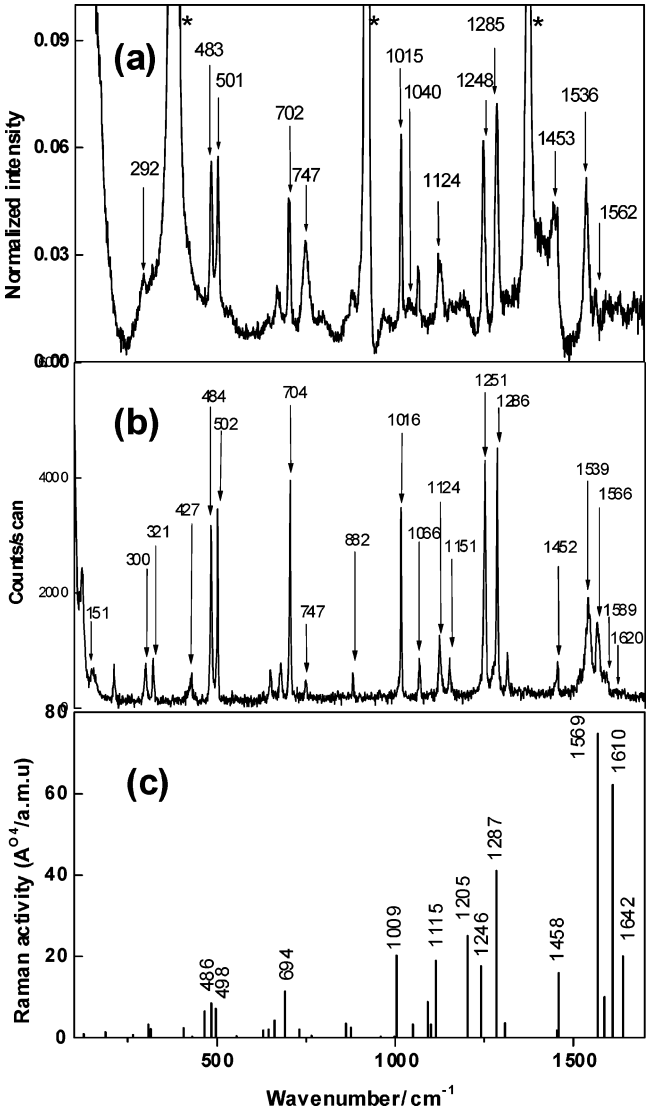

Figure 2. Normal Raman spectra of 2-ABT (a) in 0.1 M solution (an asterisk denotes the solvent band) and (b) in the solid state for $\lambda_{exc} =$ 514.5 nm. (c) shows the theoretical gas-phase Raman intensities calculated using the RHF ab initio method.

Considering the entire concentration-dependent profile, we find that the concentration range between 1.0×10^{-3} and 1.0×10^{-6} M is most sensitive not only for large signal counts but also for interesting variations in the relative intensities and band frequencies. Significant band broadening are observed for the ring breathing mode in the SERS spectra at 1.0×10^{-3} and 1.0×10^{-4} M adsorbate concentrations. It is characterized by the appearance of a blue-shifted 1027 cm^{-1} mode along with a 1019 cm^{-1} band. The concommitance of both these modes may indicate the existence of two types of adsorbed species, namely, "M" and "N", on the colloidal silver particles at these concentrations. The 1019 and 1027 cm^{-1} bands are ascribed to the breathing vibrations of the benzene moiety of the M and N species of 2-ABT, respectively.[45] The adsorption of the M species of 2-ABT involves insignificant or no interaction of the benzene ring moiety in the adsorption process. The N species on the other hand involve strong interaction of the benzene ring in the adsorption mechanism. With a decrease in concentration, the 1027 cm^{-1} band increases in intensity, and at 1.0×10^{-6} M, it is further blue shifted and appears as a single well-resolved intense band at 1031 cm^{-1} with the disappearance of the 1019 cm^{-1} mode.

The disappearance of the 1019 cm^{-1} band in the SERS spectra at 1.0×10^{-6} M can be substantiated from Figure 5, which

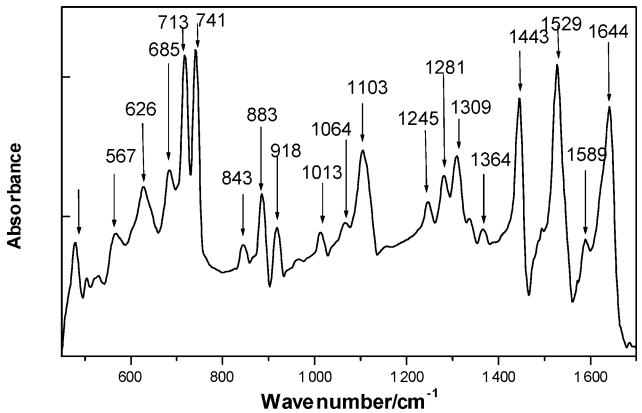

Figure 3. FTIR spectrum of 2-ABT as a neat powder in a KBr pellet.

TABLE 2: Observed and Calculated Raman and IR Bands of 2-ABT and the 2-ABT−Ag(I) Complex in Varied Environments and Their Tentative Assignments[a]

FTIR (obsd)	NRS solid (obsd)	NRS solid (calcd) RHF	NRS solid (calcd) DFT	NRS soln	SERS (10^{-4} M)	Ag complex (obsd)	Ag complex (calcd) RHF	Ag complex (calcd) DFT	tentative assignment	probable tensor element	symmetry species
1644 vs		1642	1642				1636	1652	NH_2 scissors		A′
1622 sh	1620 vvw	1610			1620 vw		1610		ν(C═N) + NH_2 scissors	α_{xx}, α_{yy}	A′
1589 sh	1589 sh	1584	1593	1588 vvw	1588 vs		1590	1596	ν(C═N) + NH_2 scissors	α_{xx}, α_{yy}	A′
	1567 s	1568	1567	1562 vvw	1574 s	1579		1584	ν(C═C)	α_{yy}	A′
1529 vs	1539 s		1550	1536 s, P			1524		NH_2 scissors		A′
1443 vs	1452 ms	1459	1456	1453 s	1451 s		1453	1449	ν(C═C)	α_{xx}, α_{yy}	A′
1309 ms	1315 ms	1307	1300		1316 vw		1327	1315	ν(C−N)	α_{zz}, α_{xy}	A′
1282 ms	1286 vs	1284	1281	1285 s, P	1288 vs	1287	1285	1281	ν(C−C)	α_{xx}, α_{yy}	A′
1245 ms	1251 vs	1245	1245	1248 s, P	1249 vs	1245	1245	1241	ν(C−C)	α_{xx}, α_{yy}	A′
	1124 s	1116	1120	1124 ms, P	1128, 1113 ms	1123	1125	1133	β(C−H)	α_{xx}, α_{yy}	A′
1103 s		1100			1100 vw				N−H deform		A′
1064 sh	1066 ms		1058	1064 ms	1070 w	1067		1064	β(C−H)	α_{zz}, α_{xy}	A′
				1040 w		1044	1043		ν(C−C)	α_{zz}, α_{xy}	A′
1014 vw	1016 vs	1007	1021	1015 s, P	1027 vs, 1019 s	1019	1007	1029 1019	ring breathing (ν_1)	α_{xx}, α_{yy}	A′
883 ms				882 w					γ(C−H)	α_{xz}, α_{yz}	A″
741 vs	747 w	735	735	747 ms, P	748 vw			760	β(C−C−C), ν_{12}	α_{zz}, α_{xy}	A′
713 vs	704 vs	697	703	702 ms, P	705 s	707	685	713	ν(C−S)	α_{xx}, α_{yy}	A′
685 w	681 ms		690								
	648 ms	660	643	667 w	653 ms	665	655	656	ν(C−S)	α_{xx}, α_{yy}	A′
	502 vs	500	494	501 s	500 ms	501	496	491	β(C−C−C)	α_{zz}, α_{xy}	A′
476 ms	484 vs	485	476	483 s		488	467				
				395 k	392 s		405		β(C−C−C), ν_{6b}	α_{xx}, α_{yy}	A′
	300 ms	309	301	293 w	286 w		287	289	γ(C−C−C)	α_{yz}, α_{xz}	A″
					217 sh	217			ν(Ag−N)		

[a] Key: β, in-plane bend; ν, stretch, γ, out-of-plane bend; vs, very strong; s, strong; ms, medium strong; w, weak; vw, very weak; vvw, very very weak; sh, shoulder; P, polarized.

TABLE 3: Apparent Enhancement Factors of Some Selected Raman Bands of 2-ABT

NRS soln band (cm^{-1})	apparent enhancement factors at various concns 1.0×10^{-3} M	1.0×10^{-4} M	1.0×10^{-5} M	1.0×10^{-6} M	1.0×10^{-7} M
501	2.59×10^2	7.72×10^3	8.57×10^4	1.44×10^6	
702	7.66×10^2	2.02×10^4	1.35×10^5	8.85×10^5	
1015	8.55×10^2	2.87×10^4	3.61×10^5	5.16×10^6	4.81×10^6
1562	2.70×10^3	7.87×10^4	7.61×10^5	8.29×10^6	

represents a bar diagram indicating the fwhm of the ring breathing mode in the NRS and SERS spectra at varied adsorbate concentrations. We observe a conspicuous increase in bandwidth of the ring breathing vibration in the SERS spectrum between 1.0×10^{-3} and 1.0×10^{-5} M with respect to its NRS counterpart in solution. The fwhm of this mode is found to drop substantially at 1.0×10^{-6} M, where it becomes almost comparable with that of its NRS counterpart.

However, a significant 16 cm^{-1} blue shift of the ring breathing in the SERS spectra in comparison with the corresponding NRS spectra of the solution, together with the disappearance of the 1019 cm^{-1} band, may indicate considerable population density of the N type of adsorbed species at 1.0×10^{-6} M concentration. The blue shift of the ring breathing mode as commonly observed in biomolecules[7,31,46−49] can be attributed to redistribution of electronic charge density in the ring as a consequence of adsorption.[50] Involvement of the fused benzene ring in the adsorption process with the decrease in concentration can be further substantiated by the increase in intensity of the 394 and 1574 cm^{-1} bands, assigned to C−C−C in-plane bending and C═C stretching, respectively. In fact, the 1574 cm^{-1} band is also blue shifted approximately ∼12 cm^{-1} compared to its NRS counterpart.

Apart from the interaction of the benzene ring of 2-ABT in the adsorption process, the fused thiazole moiety of the molecule can also bind to the silver surface through the lone pair electrons of either the nitrogen or sulfur atom or through both of them. A more favored adsorptive site can be enumerated theoretically by estimating the partial atomic charges on each of these probable active sites.[6,7] The higher the negative charge density on the atom, the higher the probability of it acting as an adsorptive site for the silver substrate. Theoretical results estimated from DFT/RHF ab initio calculations show that the partial atomic charges on the nitrogen and sulfur atoms determined by the natural population analysis (NPA) are −0.49232/−0.60133 and 0.32772/0.33512, respectively. The negative charge density is thus observed to be more appreciable on the nitrogen atom than on the sulfur atom, thereby indicating the active involvement of the nitrogen atom in the adsorption process. The appearance of a shoulder at around 217 cm^{-1} in the concentration-dependent SERS spectral profile, ascribed to the Ag−N stretching vibration,[8,51−53] indicates that the fused thiazole moiety of the 2-ABT molecule is indeed adsorbed through the ring nitrogen atom. An interesting observation can be drawn regarding the 706 cm^{-1} band present in all the concentration-dependent SERS spectra. This band, ascribed to the C−S stretching vibration,[38,40] exhibits essentially the same frequencies and band shapes in the adsorbed- and bulk-phase environments. This evidence further substantiates insignificant involvement of the sulfur atom in the adsorption process.

The lone pair electrons on the nitrogen atom of the externally attached $-NH_2$ group can also be the possible active site in the adsorption mechanism. The partial atomic charge on this nitrogen atom determined by NPA according to DFT and RHF ab initio calculation is −0.83588 and −0.90594, respectively. In the concentration-dependent SERS spectra, we observed

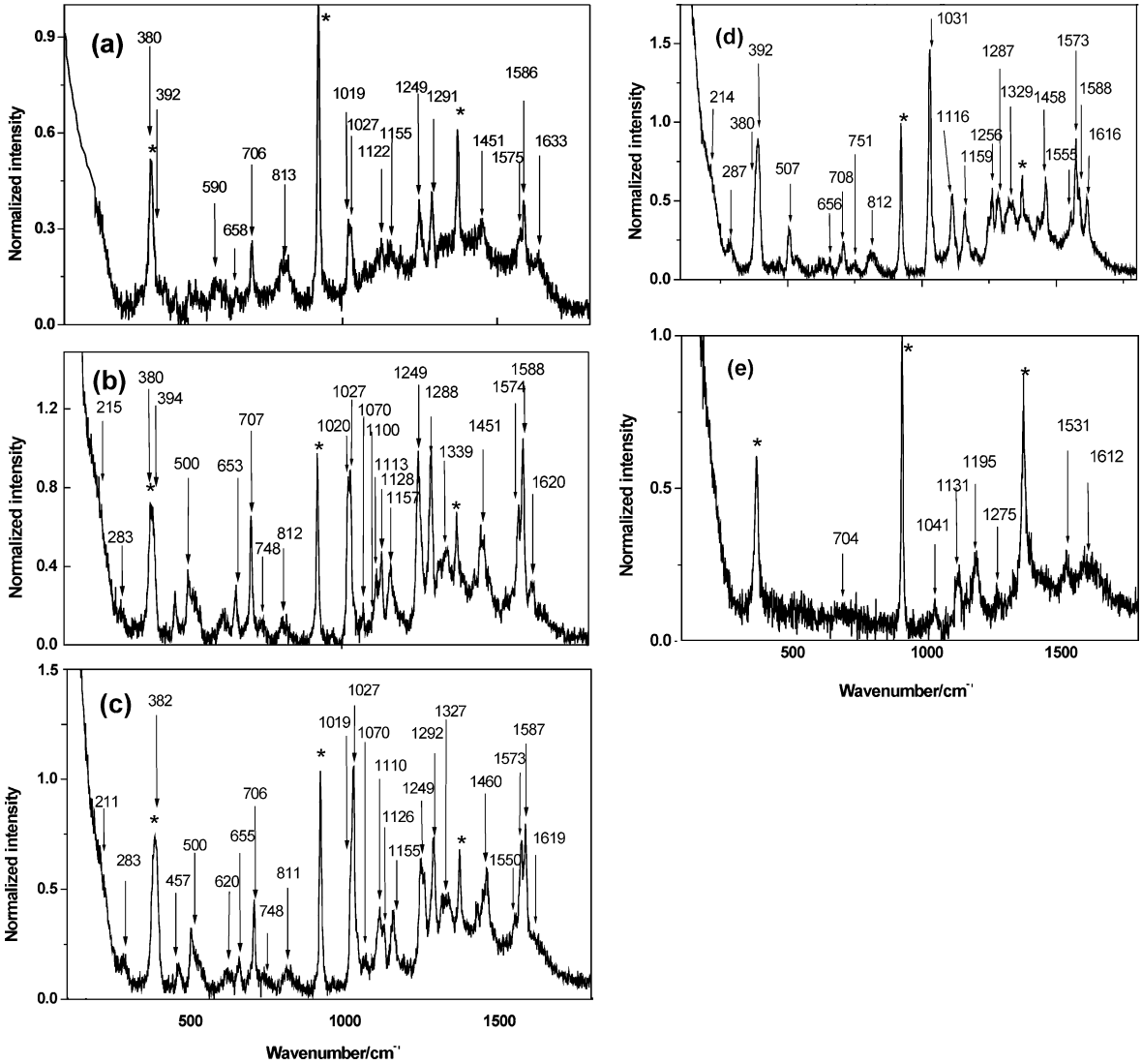

Figure 4. Normalized SERS spectra of 2-ABT in a silver hydrosol at concentrations (a) 1.0×10^{-3} M, (b) 1.0×10^{-4} M, (c) 1.0×10^{-5} M, (d) 1.0×10^{-6} M, and (e) 1.0×10^{-7} M for $\lambda_{exc} = 514.5$ nm (an asterisk denotes the solvent band).

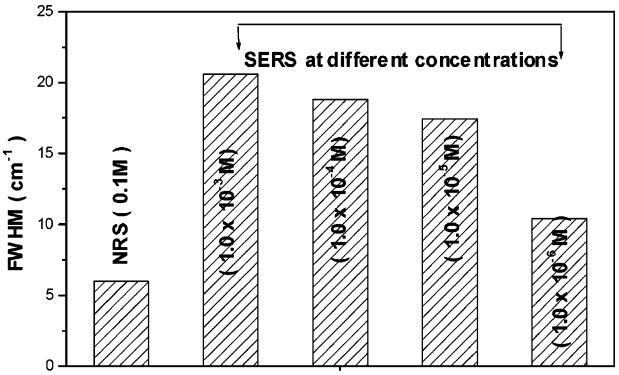

Figure 5. Bar diagram indicating the fwhm of the ring breathing (1019 cm^{-1}, i.e., ν_{12}) mode in NRS and SERS spectra.

considerable enhancement and variation in the intensity of the bands around 1550, 1588, and 1620 cm^{-1} ascribed to the $-NH_2$ scissoring mode. This may signify some interaction of the nitrogen atom of the $-NH_2$ group with the silver surface. However, among these vibrations, the 1588 and 1620 cm^{-1} bands are known to be overlapped with the C═N stretching mode of the thiazole moiety of 2-ABT.[35−38,54] So the enhancement and intensity variation of these modes may be due to the resultant interaction involving the nitrogen atom of the $-NH_2$ group and the thiazole moiety of the 2-ABT molecule. The N−H stretching modes as often reported in the 3300−3400 cm^{-1} wavenumber range[7,42] are however not observed in the concentration-dependent SERS spectra, probably due to the intense broad background of the OH stretching mode (centered around 3400 cm^{-1}) of bulk water. The N−H stretching vibration may therefore be completely masked by this intense broad background and hence could not be identified separately. The involvement of both the endocyclic and exocyclic nitrogen atoms in the adsorption process may result in the appearance of a broad shoulder in the SERS spectra at ∼217 cm^{-1}.

The relative enhancement of the Raman bands of 2-ABT on the adsorbate concentration has been estimated. Figure 6 shows the variation of the normalized SERS signal intensities of the 703, 1019, 1573, and 1583 cm^{-1} bands with the logarithm of concentration. It is observed that the SERS signal for two pairs of bands at 703 and 1583 cm^{-1} and at 1019 and 1573 cm^{-1} increase in intensity as the concentration of the adsorbate molecule is lowered, attaining a maximum at 1.0×10^{-4} and 1.0×10^{-6} M, respectively. The former pair of bands at 703 and 1583 cm^{-1} represents vibrational signatures principally contributed by the thiazole ring, while the latter pair at 1019 and 1573 cm^{-1} represents the contribution from the benzene ring of 2-ABT. It is now well established that, on silver island

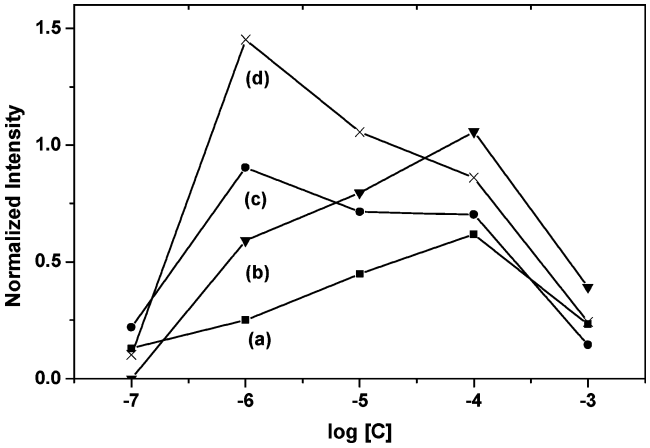

Figure 6. Concentration dependence of the intensity of the (a) 707, (b) 1587, (c) 1573, and (d) 1020 cm^{-1} SERS bands of 2-ABT.

films[55] and on silver colloids,[4,6] maximum enhancement is observed when a monolayer of adsorbate molecule is formed on the surface, and that, as multilayers are formed, the SERS signal decreases. It therefore seems plausible that the monolayer of the adsorbed 2-ABT is formed on the colloidal silver surface at two different adsorbate concentrations, which show maximum enhancement of the SERS signal.

4.3. Orientation of the 2-ABT Molecule on the Silver Surface. To have a precise idea regarding the orientation of 2-ABT at different adsorbate concentrations, we estimate the apparent enhancement factors (AEFs) of some selected Raman bands using the relation we used before[4,6,7] Accordingly

$$\mathrm{AEF} = \sigma_{\mathrm{SERS}}[C_{\mathrm{NRS}}]/\sigma_{\mathrm{NRS}}[C_{\mathrm{SERS}}] \qquad (1)$$

where C and σ represent the concentration and the peak area of the Raman bands measured from the baseline. They are shown in Table 3. The orientation of the molecule has been estimated following the surface selection rule, as predicted by Moskovits[56] and Creighton.[57] According to this rule, those vibrations having a larger component of polarizability in the direction normal to the surface will be enhanced more.

If the 2-ABT molecule is considered to be lying in the *xy* plane where *x* and *y* correspond to the long and short axes of the molecule and *z* is perpendicular to the molecular plane, then for edge-on adsorption, the vibration of the in-plane A′ species transforming as *yy* (when the short axis of the molecule is vertical to the surface) or *xx* (when the long axis of the molecule is vertical to the surface) is expected to undergo significant enhancement. The least intense band should belong to the out-of-plane A″ species transforming as *yz* and *xz*.

It is clearly seen from Table 3 that we obtain a moderate 3−4 orders of magnitude enhancement of all the bands principally representing in-plane vibrations of the A′ species at an adsorbate concentration of 1.0×10^{-4} M. The enhancement factor increases by 1−3 orders of magnitude at 1.0×10^{-6} M concentration. No significant enhancement contributed by the out-of-plane vibrations of the A″ species of the molecule are recorded. Moreover, other in-plane modes at around 392, 1588, and 1620 cm^{-1}, whose exact enhancement could not be predicted, are also significantly enhanced.

These results together with the appearance of the Ag−N stretching vibration suggest that 2-ABT molecules are adsorbed onto the metal surface through the nitrogen atoms of the thiazole moiety and also possibly through the externally attached amino group, with the molecular plane nearly vertical to the surface at all adsorbate concentrations.

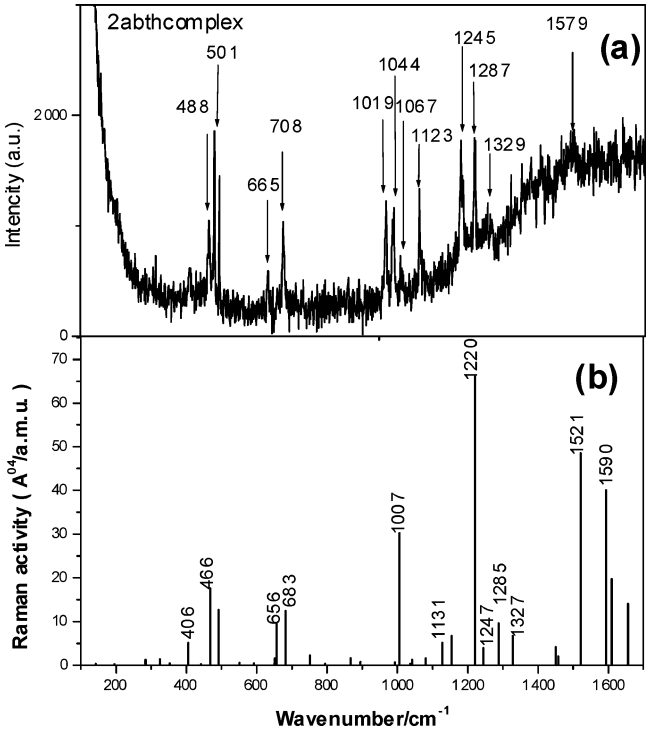

Figure 7. Normal Raman spectrum of (a) the 2-ABT−Ag(I) complex in a neat solid for $\lambda_{\mathrm{exc}} = 514.5$ nm. (b) is the theoretical gas-phase Raman intensities of the 2-ABT−Ag(I) model calculated using the RHF ab initio method.

The M-type species that are prevalent between 1.0×10^{-3} and 1.0×10^{-5} M adsorbate concentrations are thought to be adsorbed vertically in such a way that the *x* axis (long axis) of the molecule remains nearly vertical to the silver surface. This type of adsorption geometry precludes any direct interaction of the benzene ring moiety with the silver surface. The N-type species that coexist at 1.0×10^{-3} to 1.0×10^{-5} M concentration and predominantly exist at 1.0×10^{-6} M are probably adsorbed vertically with the *y* axis (the short axis) of the molecule almost normal to the silver surface. This type of adsorption favors the direct involvement of the benzene ring moiety with the silver surface.

Different forms of vertical adsorption geometry of the M and N species and their relative population in the colloidal silver surface may result in monolayer coverage of the 2-ABT molecule at two different adsorbate concentrations as observed in Figure 6.

4.4. NRS of the 2-ABT−Ag Complex. Figure 7a shows the NRS spectrum of the 2-ABT−Ag (I) complex. Well-resolved Raman bands whose vibrational signatures resemble very well those of the SERS spectrum of the molecule characterize the Raman spectrum of the complex. The Ag−N stretching vibration at 215 cm^{-1} is well identified, indicating considerable metal−adsorbate interaction. An interesting conclusion can be drawn regarding the appearance of the ring breathing mode at around 1019 cm^{-1}. The unique appearance of this band suggests insignificant interaction of the benzene ring moiety in the adsorption process. Thus, the binding arrangement of the 2-ABT−Ag(I) complex closely mimics that of the M-type adsorbed species of the SERS spectrum.

The theoretical gas-phase Raman spectrum of the modeled 2-ABT−Ag complex is shown in Figure 7b. The optimized geometries of the modeled 2-ABT−Ag(I) complex obtained from the DFT and RHF ab initio levels of theory are shown in parts a and b, respectively, of Figure 8. As one can see from

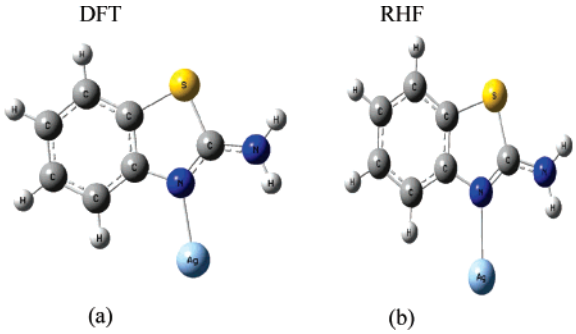

Figure 8. Optimized geometritics of the modeled 2-ABT−Ag(I) complex obtained from the (a) DFT and (b) RHF ab initio levels of theory.

Figure 7 and also from Table 2, the theoretically predicted frequencies almost matches the experimental results within a tolerable limit.

This immediately allows us to investigate the changes in the structural parameters of the 2-ABT molecule as a result of the Ag interaction. They are listed in Table 1. These parameters may be closely related to the molecular geometry of the M-type adsorbed species of the 2-ABT molecule.

5. Conclusion

The adsorption behavior of biologically significant 2-aminobenzothiazole molecules on colloidal silver particles has been investigated by SERS spectroscopy aided by density functional theory and ab initio restricted Hartree−Fock computation of vibrational frequencies of the isolated molecule. The optimized structural parameters of the free and modeled adsorbed molecule have been estimated from the above-mentioned level of theory. Some vibrational modes of the free molecule have been reassigned. The existences of two types of adsorbed species has been inferred from the concentration-dependent SERS spectral profile. The orientations of the two adsorbed species have been estimated from the surface selection rule. The Raman vibrational bands of one type of adsorbed species closely resemble those of the NRS spectrum of the chemically prepared and theoretically modeled 2-ABT−Ag(I) coordination compound.

Acknowledgment. We thank Prof. P. K. Mallick of the Physics Department, Burdwan University, Dr. S. Raychowdhury of the Chemistry Department, Dinabandhu Andrews College, Kolkata, and Prof. T. Tanaka of the Life Science Department, Kobe University, Japan, for constructive suggestions. J.C. thanks the University Grants Commission (UGC), Government of India, for financial support through a minor research project (MRP Project No. PSW-089/03-04).

References and Notes

(1) Maher, R. C.; Cohen, L. F.; Etchegoin, P. *Chem. Phys. Lett.* **2002**, *352*, 378.
(2) Nie, S.; Emory, S. R. *Science* **1997**, *275*, 1102.
(3) Bukowska, J. *J. Mol. Struct*. **1992**, *275*, 151.
(4) Chowdhury, J.; Ghosh, M.; Misra, T. N. *J. Colloid Interface Sci.* **2000**, *228*, 372.
(5) Cotton, T. M.; Aclphans, R.; Mobins, D. *J. Phys. Chem.* **1986**, *90*, 6071.
(6) Chowdhury, J.; Ghosh, M.; Misra, T. N. *Spectochim. Acta, A* **2000**, *56*, 2107.
(7) Chowdhury, J.; Mukherjee, K. M.; Misra, T. N. *J. Raman Spectrosc.* **2000**, *31*, 427.
(8) Aroca, R. F.; Clavijo, R. E.; Halls, M. D.; Schlegel, H. B. *J. Phys. Chem. A* **2000**, *104*, 9500.
(9) Bolboaca, M.; Iliescu, T.; Paizs, Cs.; Irimie, F. D.; Kiefer, W. *J. Phys. Chem. A* **2003**, *107*, 1811.
(10) Baia, M.; Baia, L.; Kiefer, W.; Popp, J. *J. Phys. Chem. B* **2004**, *108*, 17491.
(11) Moskovits, M. *Rev. Mod. Phys.* **1985**, *57*, 783.
(12) Campion, A.; Kambhampati, P. *Chem. Soc. Rev.* **1998**, *27*, 241.
(13) Chang, R. K.; Furtak, T. E. In *Surface Enhanced Raman Scattering*; Plenum Press: New York, 1982.
(14) Garcia-Vidal, F. J.; Pendry, J. B. *Phys. Rev. Lett.* **1996**, *77*, 1163.
(15) Sanchez-Gil, J. A.; Garcia-Ramos, J. V. *Chem. Phys. Lett.* **2003**, *367*, 361.
(16) Lombardi, J. R.; Birke, R. L.; Lu, T.; Xu, J. *J. Chem. Phys.* **1986**, *84*, 4174.
(17) Arenas, J. F.; Fernandez, D. J.; Soto, J.; Lopes-Tacon, I.; Otero, J. C. *J. Phys. Chem. B* **2003**, *107*, 13143.
(18) Weiss, A., Haran, G. *J. Phys. Chem. B* **2001**, *105*, 12348.
(19) He, H. W.; Mens, L. P.; Hu, L. M.; Liu, Z. J. *Chin. J. Pestic. Sci*. **2002**, *4*, 14.
(20) Elderfield, R. C. *Heterocyclic Compounds*; John Wiley and Sons, Inc.: New York, London, 1956; Vol. 5, p 487.
(21) Vara-Prasad, J. V. N.; Panapoulous, A.; Rubin, J. R. *Tetrahedron Lett.* **2000**, *41*, 4065.
(22) Witte, E. G.; Phillip, H.; Vereecken, H. *Org. Geochem*. **1998**, *29*, 1829.
(23) Kloskowski, R.; Fuehr, F. *Environ Sci. Health B* **1987**, *22*, 6.
(24) Creighton, J. A.; Blatchford, C. G.; Albrecht, M. G. *J. Chem. Soc., Faraday Trans.* **1979**, *275*, 790.
(25) Dash, R. N.; Ramana Rao, D. V. *J. Indian Chem. Soc*. **1974**, *LI*, 787.
(26) Frisch, M. J.; Trucks, G. W.; Schiegel, H. B.; Scuseria, G. E.; Robb, M. A.; Cheeseman, J. R.; Zakrzewski, V. G.; Montgomery, J. A., Jr.; Stratmann, R. E.; Burant, J. C.; Dapprich, S.; Millam, J. M.; Daniels, A. D.; Kudin, K. N.; Strain, M. C.; Farkas, O.; Tomasi, J.; Barone, V.; Cossi, M.; Cammi, R.; Mennucci, B.; Pomelli, C.; Adamo, C.; Clifford, S.; Ochterski, J.; Petersson, G. A.; Ayala, P. Y.; Cui, Q.; Morokuma, K.; Malick, D. K.; Rabuck, A. D.; Rahgavachari, K.; Foresman, J. B.; Cioslowski, J.; Ortiz, J. V.; Stefanov, B. B.; Liu, G.; Liashenko, A.; Piskorz, P.; Komaromi, I.; Gomperts, R.; Martin, R. L.; Fox, D. J.; Keith, T.; Al-Laham, M. A.; Peng, C. Y.; Nanayakkara, A.; Gonzalez, C.; Challacombe, M.; Gill, P. M. W.; Johnson, B. G.; Chen, W.; Wong, M. W.; Andres, J. L.; Head-Gordon, M.; Replogle, E. S.; Pople, J. A. *Gaussian 98*; Gaussian, Inc.: Pittsburgh, PA, 1998.
(27) Perdew, J. P.; Wang, Y. *Phys. Rev. B* **1992**, *45*, 13244.
(28) Frisch, M. J.; Pople, J. A.; Binkley, J. S. *J. Chem. Phys*. **1984**, *80*, 3265.
(29) Scott, A. P.; Radom, L. *J. Phys. Chem.* **1996**, *100*, 16502.
(30) EL-Azhary, A. A. *Spectrochim. Acta, A* **1999**, *55*, 2437.
(31) Giese, B.; McNaughton, D. *J. Phys. Chem. B* **2002**, *106*, 101.
(32) Pergolese, B.; Bigotto, A. *J. Raman Spectrosc*. **2002**, *33*, 646.
(33) Mukherjee, K.; Sanchez-Cortes, S.; Garcia-Ramos, J. V. *Vib. Spetrosc.* **2001**, *25*, 91.
(34) Koglin, K.; Witte, E. G.; Meier, R. J. *Vib. Spectrosc*. **2003**, *33*, 49.
(35) Pannizzi, J. C.; Davidovics, G.; Guslielmetti, R.; Mille, G.; Metzger, J. Cnouteau, J. *Can. J. Chem.* **1971**, *49*, 956.
(36) Collier, W. B.; Klots, T. D. *Spectrochim. Acta, A* **1995**, *51*, 1255.
(37) Klots, T. D.; Collier, W. B. *Spectrochim. Acta, A* **1995**, *51*, 1273.
(38) Mohan, S.; Prabakar, A. R.; Prameela, S. *Indian J. Pure Appl. Phys.* **1999**, *29*, 672.
(39) Pergolese, B.; Bigotto A. *J. Raman Spectrosc.* **2003**, *34*, 84.
(40) Sandhyarani, N.; Skanth, G.; Berchmans, S.; Yegnaraman, V.; Pradeep, T. *J. Colloid Interface Sci.* **1999**, *209*, 154.
(41) Bohlig, H.; Ackermann, M.; Billes, F.; Kundra M. *Spectrochim. Acta, A* **1999**, *55*, 2635.
(42) Varsanyi, G. *Vibrational spectra of benzene derivatives*; Academic Press: New York, London, 1969.
(43) Wait, S. C.; Mcnerney, J. C. *J. Mol. Spectrosc.* **1970**, *34*, 56.
(44) (a) Chowdhury, J.; Ghosh, M. *J. Colloid Interface Sci.* **2004**, *277*, 121. (b) Chowdhury, J.; Ghosh, M. *J. Raman Spectrosc.* **2004**, *35*, 1023.
(45) Gao, P.; Weaver, M. J. *J. Phys. Chem.* **1985**, *89*, 5040.
(46) Sanchez-Cortes, S.; Garcia-Ramos, J. V. *Vib. Spectrosc*. **1993**, *4*, 185.
(47) Oh, W. S.; Kim, M. S.; Suh, S. W. *J. Raman Spectrosc.* **1987**, *18*, 253.
(48) Kim, S. K.; Joo, T. H.; Suh, S. W.; Kim, M. S. *J. Raman Spectrosc.* **1986**, *17*, 381.
(49) Giese, B.; Mc. Naughton, D. *Phys. Chem. Chem. Phys*. **2002**, *4*, 5171.
(50) Comfeita, L. E.; Sanchez-Cortes, S.; Garcia-Ramos, J. V. *J. Raman Spectrosc.* **1995**, *26*, 149.
(51) Boo, D. W.; Kim, M. S.; Kim, K. *Bull. Korean Chem. Soc*. **1988**, *9*, 311.
(52) Miranda, M. *J. Raman Spectrosc.* **1997**, *28*, 205.
(53) Miranda, M. *Chem. Phys. Lett*. **2001**, *340*, 437.
(54) Lagranse, C. G.; Cnouteau, J.; Metzger, J. *Spectrochim. Acta* **1967**, *23A* 1477.
(55) Sanda, P. N.; Warlaumont, J. M.; Dermuth, J. E.; Tsang. J. C.; Christmann, T.; Bradley, J. A. *Phys. Rev. Lett.* **1980**, *45*, 1519.
(56) Moskovits, M. *J. Chem. Phys*. **1982**, *77*, 4408.
(57) Creighton, J. A. *Surf. Sci.* **1983**, *124*, 209.